

Recovery and Reuse of Composite Cathode Binder in Lithium Ion Batteries

Amrita Sarkar,^[a, b] Richard May,^[a] Sapna Ramesh,^[a] Wesley Chang,^[c] and Lauren E. Marbella^{*[a]}

Here, we investigate the recovery and reuse of polyvinylidene fluoride (PVDF) binders from both homemade and commercial cathode films in Li ion batteries. We find that PVDF solubility depends on whether the polymer is an isolated powder or cast into a composite film. A mixture of tetrahydrofuran:N-methyl-2-pyrrolidone (THF:NMP, 50:50 v/v) at 90 °C delaminates composite cathodes from Al current collectors and yields pure PVDF as characterized by ¹H nuclear magnetic resonance (NMR), gel

permeation chromatography (GPC), wide-angle X-ray scattering (WAXS), and scanning electron microscopy (SEM). PVDF recovered from Li ion cells post-cycling exhibits similar performance to pristine PVDF. These data suggest that PVDF can be extracted and reused during Li ion battery recycling while simultaneously eliminating the formation of HF etchants, providing an incentive for use in direct cathode recycling.

1. Introduction

The market for electric vehicles (EVs) has expanded dramatically in the past several years in a collective effort to combat the greenhouse gas emissions associated with climate change.^[1] By 2040, 500 million passenger EVs are expected to be on the road, all of which will likely be powered by lithium-ion batteries (LIBs).^[1,2] As a result, we will face an unprecedented amount of LIB waste in the near future.^[3,4] Recycling efforts focused on mitigating the environmental impact and hazards of this waste as well as improving the reuse of battery materials for subsequent applications are critical.

Ultimately, LIB recycling procedures that recover and reuse every component of the battery are ideal and would match standards already in place for lead-acid batteries.^[3,4] LIB recycling techniques are comparatively nascent and thus, strategies have focused on recovering the most valuable components (e.g., Co) from cathode films. For example, pyrometallurgy and hydrometallurgy processes use high temperature and/or chemical leaching to extract Co²⁺ and Ni²⁺ from composite cathodes.^[5–17] However, these processes are low

value, producing raw salt precursors that require resynthesis of the active cathode materials (usually a layered transition metal oxide, e.g., LiCoO₂ (LCO), LiNi_xMn_yCo_zO₂ (NMC), or LiNi_xCo_yAl_zO₂ (NCA)).^[4,18–20] Thus, more recent research efforts have focused on direct cathode recycling, where the active material is recovered directly from the cathode composite for immediate reuse in subsequent battery applications.^[3,21–26] In direct cathode recycling, the active material is separated from the conductive carbon, the polyvinylidene fluoride (PVDF)-based binder, and the Al current collector via pyrolysis,^[12–14,18,19,27–30] leading to incineration of carbon and polymeric binder.^[26]

In particular, pyrolysis of PVDF forms a variety of potent greenhouse gases and other chemical hazards such as HF and perfluorocarbons,^[31–37] the former of which must be captured by acid scrubbers at recycling plants even though they only make up a small portion of the overall composite mass.^[38–40] Further, the formation of HF during pyrolysis deactivates layered cathode materials, leading to poor electrochemical performance^[41] and necessitating subsequent relithiation.^[42] Thus, there is a substantial motivation to remove PVDF during direct cathode recycling.


The most common approach to remove PVDF at the lab scale is through solvent-based approaches.^[41–45] The reuse of polymeric materials is notoriously challenging and has ultimately contributed to our dire plastic pollution epidemic.^[46–48] Therefore, while several different solvent systems have been explored in the literature, there has not been a systematic study on PVDF solubility nor the potential for reuse to date.


Here, we report on the solubility behavior of PVDF in both powdered form and composite cathode films (homemade and commercial Samsung 18650). We present a complete characterization of polymer binder physical properties post-recovery using nuclear magnetic resonance (NMR) spectroscopy, gel permeation chromatography (GPC), wide-angle X-ray scattering (WAXS), scanning electron microscopy (SEM), and powder X-ray diffraction (PXRD). The performance of recovered PVDF in subsequent Li-ion battery composite cathodes is evaluated

[a] Dr. A. Sarkar, R. May, S. Ramesh, Prof. L. E. Marbella
Department of Chemical Engineering
Columbia University
New York, NY 10027 (USA)
E-mail: lem2221@columbia.edu

[b] Dr. A. Sarkar
Department of Chemistry and Biochemistry
Montclair State University
Montclair, NJ 07043 (USA)

[c] W. Chang
Department of Mechanical Engineering and Material Science
Princeton University
Princeton, NJ 08544 (USA)

 Supporting information for this article is available on the WWW under <https://doi.org/10.1002/open.202100060>

 © 2021 The Authors. Published by Wiley-VCH GmbH. This is an open access article under the terms of the Creative Commons Attribution Non-Commercial License, which permits use, distribution and reproduction in any medium, provided the original work is properly cited and is not used for commercial purposes.

together with an energy intensity analysis to describe the economics associated with binder recycling.

2. Results and Discussion

2.1. PVDF Solubility Behavior for Recovery from Composite Cathode Films

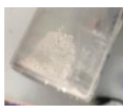






We investigated a range of pure and binary organic solvents to solubilize PVDF-containing powders and films including dimethylformamide (DMF), N-methylpyrrolidone (NMP), tetrahydrofuran (THF), and mixtures thereof (Table 1). For PVDF recovery from composite cathode films, both homemade and commercial composite cathode films were cut into pieces and suspended in the solvent at 90 °C for 1.5 h to evaluate the extent of PVDF dissolution (see experimental details, and supporting information, S1.1–S1.5, Table S1–S2). In these solubility tests, commercial films underwent long term cycling prior to PVDF recovery (Figures S1–S2). After delamination, the reaction mixture was fed through an alumina column to separate the polymeric binder from the active materials, carbon black, and Al current collector (Figure S3).

Although pristine PVDF was soluble in all of the organic solvents tested (DMF, NMP, THF, THF:NMP 80:20, THF:DMF 80:20, THF:NMP 50:50, THF:DMF 50:50), only a subset of these solvents were able to dissolve PVDF from composite cathode films on Al substrates (DMF, NMP, THF:NMP 50:50, THF:DMF 50:50). PVDF films recovered from DMF-containing solutions were more yellow in color (Table 1), suggesting that DMF (or impurities in DMF) alters the physical properties of the

polymer (pristine PVDF is a white powder). Conversely, THF, NMP, and mixtures thereof led to clear/white films. Table 1 shows that the color of recovered PVDF strongly depends on the solvent used for extraction as well as treatment conditions. For example, the PVDF recovered from the Samsung batteries is darker (Figure S5) than our homemade films, suggesting the presence of minor impurities post-cycling, such as residual carbon black, PVDF copolymers, minor impurities in solvents, or changes in the material from electrochemical cycling.^[49–53] We expect that the PVDF used in commercial cells may also differ slightly in molecular weight or structure (e.g., a PVDF copolymer, such as PVDF-HFP (poly(vinylidene fluoride-co-hexafluoropropylene)), or poly(vinylidene fluoride-co-chlorotrifluoroethylene) (PVDF-CTFE)).^[49,50]

While pure NMP has been used previously to remove PVDF from composite films,^[29,30,42,54] we found that the addition of more volatile THF allowed us to readily remove solvent. Thus, a THF:NMP (50:50 v/v) binary solvent mixture was used for all subsequent PVDF recovery experiments. PVDF recovery yields of $81 \pm 3\%$ and $69 \pm 3\%$ were achieved for homemade composite LCO and NMC111 films, respectively, upon precipitation and solvent removal (Table 2, Table S2). Similarly, commercial composite films extracted from Samsung batteries showed a PVDF recovery of $62 \pm 5\%$ for cells cycled at 1 C for 920 cycles at 40 °C (Cell A) prior to disassembly. Cell B was cycled at 1 C for 792 cycles at 5 °C and showed PVDF recovery values of $74 \pm 5\%$. In total, the percent recovery range spans from 60–80% and may depend on prior conditions. PVDF loss during recovery is primarily attributed to the alumina column/flask and not residual PVDF on the active material based on the

Table 1. PVDF binder solubility in organic solvents and binary mixtures.

PVDF Type	THF only	DMF only	NMP only	THF + NMP (80:20) (v/v)	THF + DMF (80:20) (v/v)	THF + NMP (50:50) (v/v)	THF + DMF (50:50) (v/v)
Pristine PVDF (MTI)	+	+	+	+	+	+	+
PVDF recovered from homemade cathode films	–	+	+	–	–	+	+
PVDF recovered from Samsung battery cathodes	–	+	+	–	–	+	+
Physical appearance of recovered PVDF							

All solubility experiments were performed with S/L ratio of 1:100 g:mL, T=90 °C.
[a] Solubility experiment conducted at T=60 °C. (–) insoluble, (+) soluble.

Table 2. Summary of PVDF recovery yields for different cathode composites and commercial batteries.

Composite cathode description	Treatment	PVDF recovery yield (%)
homemade LCO composite	soaked in LP30 for 48 h in an Ar glovebox at RT	81 ± 3
homemade NMC 111 composite	soaked in LP30 for 48 h in an Ar glovebox at RT	69 ± 10
Samsung 18650 (2600 mAh) Cell A	(920 cycles @ 40 °C), after long-term cycling at 1 C CC charge and discharge	$62 \pm 5^{[a]}$
Samsung 18650 (2600 mAh) Cell B	(792 cycles @ 5 °C), after long-term cycling at 1 C CCCV charge and CC discharge	$74 \pm 5^{[a]}$

[a] This number assumes the composite cathode from the commercial cell contains 3% PVDF. Commercial cells typically contain 2–4% binder. Error bars represent the standard deviation of the average for N=3–4 measurements.

fact that pristine active materials are observed in SEM analyses (Figure S24).

2.2. PVDF Post-Recovery Characterization

PVDF recovered from the composite cathodes listed in Table 2 was characterized by ^1H NMR, GPC, WAXS, and SEM and compared to pristine PVDF (i.e., the same PVDF that was used to make our homemade composite films from MTI).

Analysis with ^1H NMR shows two resonances, one at 2.88 and one at 2.27 ppm (Figure 1) that are assigned to head-to-tail (ht) and tail-to-tail (tt) bonding arrangements of vinylidene fluoride units^[55] in PVDF. The dotted line drawn through these peaks, comparing pristine PVDF to PVDF recovered from cathode films, shows that the molecular structure of PVDF remains intact after recovery. A small, high frequency shift (2.89 ppm) is observed for the ^1H ht resonance between the

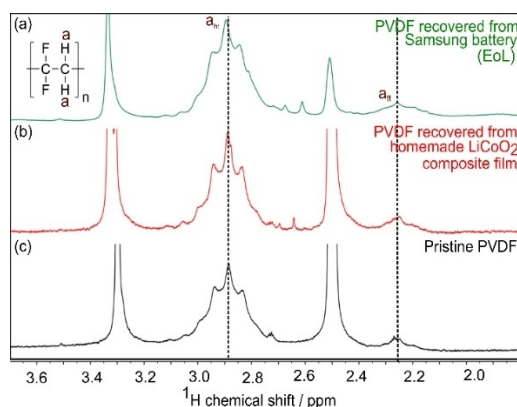


Figure 1. ^1H NMR spectra recorded in $\text{DMSO}-d_6$ of PVDF recovered from a commercial Samsung 18650 battery (Cell A, 920 cycles at 40°C) (a), a homemade LCO composite film (soaked in LP30 electrolyte for 48 h) (b), and pristine PVDF (c). The strong (cut off) peaks at 2.51 and 3.30 ppm are due to residual DMSO and HDO in the NMR solvent, respectively. Minor peaks between 2.60–2.70 ppm come from residual NMP.

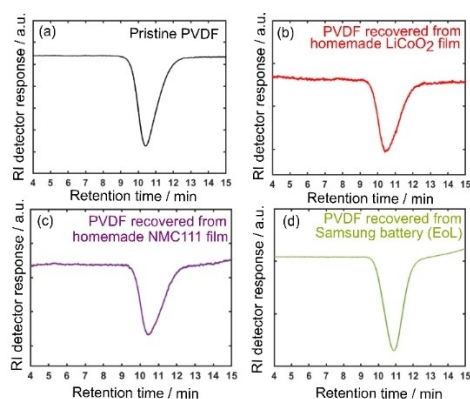


Figure 2. Refractive index (RI) GPC traces of commercially-purchased pristine PVDF (a), PVDF recovered from homemade composite LCO (b) and NMC111 films soaked in LP30 electrolyte for 48 h (c), and a commercial Samsung battery (Cell A, 920 cycles at 40°C) (d). Due to the lower refractive index of PVDF than GPC eluent ($\text{DMF} + 0.1 \text{ wt\% LiBr}$), negative GPC profiles were detected.

PVDF recovered from commercial films when compared to pristine PVDF. While this may be a result of small changes in PVDF structure, it is more likely that the binder used in industry to fabricate commercial cells has a slightly different molecular structure than the pristine PVDF used in our laboratory. The ^1H NMR recovered from two different Samsung cells (Cell A and Cell B) was nearly identical (Figure S13) and thus, all subsequent characterizations focus on Cell A.

GPC elugrams for pristine PVDF and PVDF recovered from homemade composite cathode films all fall in the same retention time range of 10.40–10.43 min (Figure 2). The pristine PVDF sample showed $M_w = 926 \text{ kg/mol}$ and $\bar{D} = 3.04$ and the PVDF recovered from homemade LCO composite film showed $M_w = 855 \text{ kg/mol}$ and $\bar{D} = 2.07$. The PVDF recovered from homemade NMC111 composite film showed $M_w = 706 \text{ kg/mol}$ and $\bar{D} = 2.54$. Molecular weights and dispersities were estimated from a calibration curve constructed from a series of polymethyl methacrylate (PMMA) standards. However, the determination of molecular weights from GPC may not be absolutely quantitative because the GPC calibrating agent, PMMA, gives positive RI signal^[56] whereas the PVDF gives a negative signal.^[57] Since the same PVDF was used for the pristine sample to prepare our homemade composite films, we conclude that the similarities in the retention times, molecular weights, and dispersities all suggest that little to no structural degradation occurs during the recovery process. PVDF recovered from Cell A after long-term cycling gave GPC elugrams with slightly higher retention time ($\sim 10.90 \text{ min}$), corresponding to average $M_w \sim 424 \text{ kg/mol}$ and $\bar{D} = 2.43$. These differences in retention times between the commercial film and the PVDF used in our laboratory are consistent with the small changes in frequency observed in ^1H NMR and suggest a slightly different structure for industrial PVDF.

WAXS of pristine PVDF powder is semicrystalline in nature (Figure 3), displaying α phase reflections at 18.5° and 20° that correspond to the (020) and (110) lattice planes.^[58–60] These reflections are retained in PVDF recovered from composite films, indicating that there are no changes in long-range order

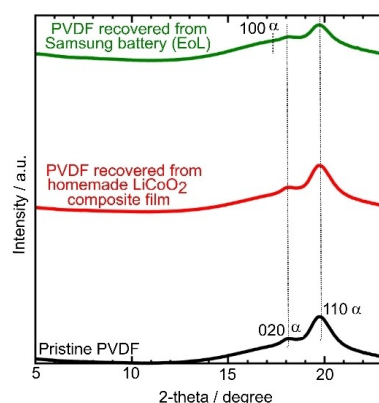


Figure 3. 1D WAXS intensity profiles of pristine PVDF powder (black) compared to PVDF recovered from homemade composite LCO films (red) and a Samsung battery (Cell A) after 920 cycles at 40°C (green). Graphs are offset vertically for clarity.

in the material upon recovery. An additional broad shoulder with a center of mass at approximately 17.5° , consistent with the (100) reflection in the α phase, is found in the PVDF recovered from the Samsung battery Cell A. No sharp reflections from LCO ($2\theta = 17.9^\circ$, Figure S14) are detected in recovered PVDF samples, suggesting that the PVDF has been separated from the active material.

The surface morphology of PVDF binder was evaluated before and after recovery with SEM (Figure S15–S16). As-received PVDF powder is comprised of primary particles with a diameter $d = 284 \pm 28$ nm (Figure S15). After recovery, PVDF shows similar primary particles with $d = 292 \pm 62$ nm as well as microscopic pores with $d = 148 \pm 54$ nm (Figure S16). Consistency in the particle size indicates that the morphology of primary PVDF particles remains intact. The observed pores/voids may arise during initial film fabrication (e.g., electrode casting and drying) and/or during the recovery and solvent evaporation process.^[61–63] Taken together, our characterizations indicate that solvent-based recovery does not substantially alter PVDF structure or morphology.

2.3. Reuse of PVDF Post-Cycling in Cathode Composites

The performance of PVDF extracted from homemade composite and commercial cells in Li/LCO half cells was compared to cells made with pristine PVDF (Figure 4). Direct comparison of batteries containing pristine PVDF (Figure 4, black squares) and PVDF recovered from homemade films and Cell A (Figure 4, red circles and green triangles) indicates that electrochemical performance is higher for recovered PVDF than pristine PVDF (65% capacity retention for pristine PVDF vs. 72% for PVDF recovered from homemade films, 76% for PVDF recovered from Cell A), providing a potential motivation to reuse PVDF from spent cells. (Note that the capacity retention values found using pristine PVDF are typical for Li/LCO half cells cycled from 2.7 to

4.2 V vs Li^+/Li).^[64] In contrast, when no binder is used, cells exhibit low capacity values almost immediately (Figure 4, orange triangles), which is consistent with work showing that binder is necessary to minimize mechanical stress in the electrode and prevent damage to the electrode microstructure.^[65,66] Average Coulombic efficiencies of cells made with all PVDF compositions is consistently $\sim 99.6\%$, while the average Coulombic efficiency of binder-free cells is slightly slower (99.3%) over 100 cycles (Figure S27). Improved performance upon reuse of polymeric materials has been observed for second-use separators.^[26] Although the reasoning for this enhancement is not completely understood, it indicates that conditioning of polymers during cycling may improve electrochemical behavior downstream. Section S2 and Figures S17–S26 provide a full description of active material recovery and characterization after solvent-based PVDF removal. We find that the active materials exhibit high purity, consistent with complete PVDF removal for subsequent use.

2.4. Feasibility of PVDF Recovery and Re-Use

Approximately 21 million tons of end-of-life battery waste will be generated by 2040.^[1,2] Although a very small percentage of polymer binder (2–4%) is used to construct a cell, battery waste of this magnitude will lead to a large accumulation of plastics from the binder, and efforts to mitigate polymer waste should be explored. Further, pyrolysis of PVDF forms HF, which degrades the active material surface, limiting the application of direct cathode recycling efforts. The recovery of PVDF with THF:NMP for the structural characterization presented here uses a solid-to-liquid (S/L) ratio of approximately 1:(115 \pm 25) g: mL (Table S2). This value facilitated ease of handling during characterization, but is higher than previously reported values in literature, with S/L ratios of 1:1.5 g:mL, 1:10 g:mL, and 1:20 g:mL achieved using heat or sonication.^[30,41,43] Large solvent volumes make PVDF recovery cost-prohibitive^[3,67–69] and thus, we explored the solubility limit of PVDF under our conditions. Using THF:NMP at the lab scale, we found that a S/L ratio of 1:(5.8 \pm 0.6) g:mL was required to achieve full delamination from the current collector (Table S3). An estimate for the energy intensity of soaking^[70,71] indicates that increasing from a S/L ratio of 1:1 to 1:5 leads to an increase in energy intensity from approximately 8 to 27 mmBtu/ton PVDF (Section S3, SI). In contrast, the energy intensity for the production of raw PVDF is estimated to be approximately 21 mmBtu/ton (based on PVC).^[67,68] These quantities suggest that in order for PVDF recycling to be economical, low S/L ratios enabled by sonication must be used, likely in tandem with direct cathode recycling efforts that recover high value active material. The solvent must be able to extract PVDF from multiple different electrodes that have undergone different practical uses during their lifetime and the relationship between PVDF solubility and electrochemical treatment should be further explored.

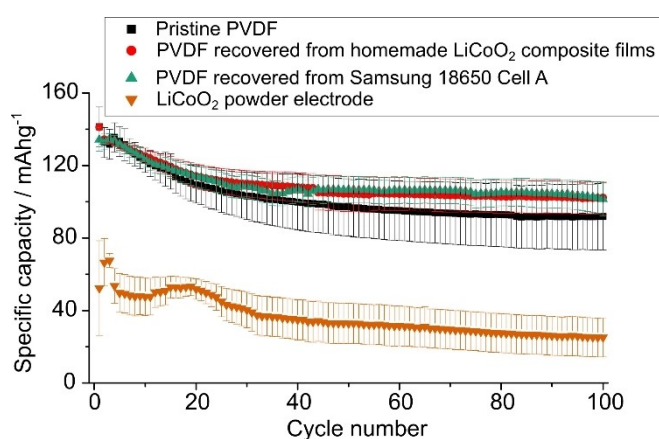


Figure 4. Specific charge capacities as a function of cycle number for Li/LiCoO₂ half cells galvanostatically cycled from 2.7 to 4.2 V vs Li^+/Li at C/10 using PVDF purchased from MTI (black squares, N = 3), PVDF recovered from homemade LiCoO₂ composite films (red circles, N = 5), PVDF recovered from 18650 Samsung Cell A (green triangles, N = 8), and cells containing no PVDF binder (orange triangles, N = 3). Error bars represent standard error.

3. Conclusion

We find that solvent-based recycling of PVDF from spent Li ion battery cathodes with THF:NMP=50:50 yields high purity PVDF that can be reused in subsequent battery applications. While the search for new, biodegradable binder materials is ongoing, PVDF-based binder remains the most commercially relevant for LIBs and thus emphasizes the need to devise strategies to handle this new source of polymeric waste. In order for PVDF recycling to be economically feasible, low S/L ratios must be used. The active material recovered from THF:NMP soaking does not suffer from HF etching and may provide an additional incentive to apply this or similar approaches.

Experimental Section

Materials

Lithium ribbon (0.75 mm thick, Sigma-Aldrich), lithium nickel manganese cobalt oxide ($\text{LiNi}_x\text{Mn}_y\text{Co}_z\text{O}_2$, $x:y:z=1:1:1$, NMC111, MTI Corporation), 1 M lithium hexafluorophosphate (LiPF_6) solution in ethyl carbonate (EC) and dimethyl carbonate (DMC) mixture (EC:DMC 1:1, v/v) (LP30, Sigma-Aldrich), N-methyl-2-pyrrolidone (NMP, anhydrous, >99%, Sigma-Aldrich) and dimethyl carbonate (DMC, anhydrous, >99%, Sigma-Aldrich) were stored in an Ar-filled glovebox ($\text{O}_2 < 0.1$ ppm, $\text{H}_2\text{O} < 0.5$ ppm) and used as received. Lithium cobalt (III) oxide (LiCoO_2 , LCO) was purchased from MTI Corporation and calcined at 800 °C in air, then stored in the glovebox prior to use. Super P conductive carbon black (C45, MTI Corporation), poly(vinylidene fluoride) binder (PVDF, MTI Corporation, >99.5%, $M_w \sim 600,000$ g/mol), tetrahydrofuran (THF, 99.5%, anhydrous, stabilized, ACROS Organics), aluminum oxide (Al_2O_3 , 99%, ACROS Organics), N,N-dimethylformamide (DMF, 99.8%, Alfa Aesar), acetonitrile (ACN, 99.7%, spectrophotometric grade, Alfa Aesar) and dimethyl sulfoxide- d_6 ($\text{DMSO}-d_6$, 99.9% atom D, Cambridge Isotope Laboratories) were stored in ambient conditions and used without further purification. Diethyl ether (anhydrous, ACS reagent, ACROS Organics) was stored at 2–8 °C.

Homemade Composite Cathode Film Fabrication and Treatment

400 mg of cathode active material (either LCO or NMC111) was hand ground in a mortar and pestle with 50 mg carbon black until a fine, uniform powder was observed. Separately, 50 mg of PVDF was dissolved in 60 drops (~1.4 mL) of NMP. LCO, carbon black, and PVDF were combined in a 80:10:10 ratio to obtain a slurry that was cast onto an Al substrate (25 μm thick) with a 300 μm doctor blade. Composite cathode films were dried on a hot plate set to 80 °C for 30 min and *in vacuo* at 100 °C for 4–6 h. Dried films were soaked in LP30 electrolyte in the glovebox for 48 h and washed twice with 15 mL DMC to remove trace amounts of electrolyte. No attempt was made to recover electrolyte components. The washed film was dried *in vacuo* overnight (12–16 h) at 60 °C and used for PVDF extraction.

Commercial Battery Disassembly

Samsung 18650 cylindrical cells rated for 2600 mAh were purchased from Amazon. Post-mortem analysis with energy dispersive

X-ray spectroscopy (EDS) indicates that the cathode is a mixture of LCO and NMC (vide infra). Two cells that had undergone approximately 6 months of long-term cycling were disassembled to investigate the recovery and subsequent re-use of PVDF described herein. The cycling protocol that each cell had undergone is depicted in Table S1. Cell A had undergone 920 cycles at a rate of 1 C (2.6 A) under constant current (CC) charge and discharge, whereas Cell B had undergone 792 cycles at a rate of 1 C under constant current constant voltage (CCCV) charge and constant current discharge. These cycling schemes are typical of long-term cycling studies for Li-ion batteries (LIBs). Cell A was cycled in a temperature chamber held at 40 °C and Cell B was cycled in a temperature chamber held at 5 °C. Sample voltage and current profiles for the first and last 25 h of cycling for each cell are depicted in Figure S1 and S2. Average Coulombic efficiencies (CEs) are calculated and shown in Table S1 (average of discharge/charge capacities for all cycles). After the long-term cycling experiments, the cells were stored at rest for approximately 10 months before disassembly. Immediately before disassembly, the cells were fully discharged to 2.7 V before transferring into the glovebox. An electric Dremel tool was used at medium power along the edge of the cells to cut open the cap and then along the side to unfurl the cylindrical container. The electrodes were unrolled, the cathode side was peeled off, washed, and processed in the same fashion as the homemade composite cathode films described above.

PVDF Recovery from Composite Cathodes Using THF:NMP (50:50 v/v)

To optimize the recovery procedure, a range of solvents, solvent mixtures, and different experimental conditions were screened for PVDF solubility and removal (see Section S1.1–S1.5, Figure S6–S10). From this process, we found that a 50:50 (v/v) mixture of THF:NMP allowed PVDF to be recovered in a form that facilitated reuse of the binder. In both homemade and commercial composite cathode films, the following procedure was used to recover PVDF binder (Figure S3). Cathode films were cut into approximately 1 cm \times 1 cm pieces and immersed in THF:NMP in a round bottom flask while stirring. Typical mass concentrations of the cathode films, including the Al substrate were 1:(115 \pm 25) g:mL (Table S2). Subsequent experiments were performed to minimize the solvent volume. The reaction flask was equipped with a condenser and set into a preheated oil bath to reflux at 90 °C. The film started to fall off in the solvent mixture after 20–30 min as the PVDF dissolved and was completely dispersed within 50 min, leaving behind bare Al substrates. The reaction was allowed to continue for 1.5 h. Next, the solution was cooled at room temperature, diluted with 5–10 \times excess THF, and passed through an alumina column (Al_2O_3 column thickness is maintained at ~1–1.5 cm). The filtrate consisted of a transparent, slightly yellow, PVDF solution in THF:NMP. In some instances, the filtrate appeared darker, possibly due to contamination from residual active material and/or carbon. These species were removed by re-filtering through a fresh alumina column to obtain the transparent PVDF solution. The PVDF solution was concentrated under vacuum to remove THF and then precipitated in chilled (in liquid N_2) anhydrous diethyl ether. The top, liquid portion was carefully decanted and discarded. The remaining viscous, opaque solution on the bottom of the vessel was evaporated under vacuum and a solid PVDF film was obtained. The resulting free-standing, dried PVDF films were weighed on an analytical balance to calculate the percent recovery. The PVDF recovery yields were cross-checked with quantitative NMR spectroscopy to ensure the mass corresponded to pure PVDF and were found to match well (Figure S4). The recovered PVDF film was characterized by ^1H NMR spectroscopy, wide angle X-ray scattering (WAXS), gel permeation chromatography (GPC), powder X-ray

diffraction (PXRD), and scanning electron microscopy (SEM). Re-use of PVDF in Li-ion batteries was also examined in subsequent experiments (vide infra). Slight differences in color of the final PVDF was noted for our homemade composites compared to the PVDF recovered from Samsung cells. Our homemade films yielded a solid, white PVDF film, whereas the PVDF recovered from commercial batteries after long-term cycling was dark yellow in color (Figure S5). PVDF recovery yields from different films and different organic solvents/solvent mixtures are listed in Table 1, and Table S2.

Solvent Minimization for PVDF Recovery

Due to the cost associated with wet chemical recycling, efforts were made to explore routes that minimize the volume of solvent required to recover PVDF from composite cathodes films while still achieving full delamination. In these experiments, a homemade LCO composite cathode film was soaked in electrolyte and a modified recovery procedure was used to extract PVDF (Figure S11). After testing several different ratios, we found that with the 50:50 THF:NMP solvent mixture, the minimal solvent-to-liquid ratio needed to completely dissolve the PVDF was $1:(5.8 \pm 0.6)$ g:mL (Table S3, Figure S12). In the modified experimental approach, dried cathode films were cut into approximately $0.5 \text{ cm} \times 0.5 \text{ cm}$ pieces and immersed into the THF:NMP binary mixture ($v/v=50:50$) in a round bottom flask. Typical mass concentrations of the cathode films, including Al substrate, were $175 \pm 18 \text{ mg/mL}$ (Table S3), which is $\sim 20\times$ more concentrated than our procedure outlined in Section S1.4. In the solvent minimization procedure, $\sim 3\text{--}4 \text{ g}$ of cathode composite is dispersed in only 20 mL of solvent. Similarly, the reaction flask was equipped with a condenser and set into a preheated oil bath at 90°C with constant vigorous stirring for 2.5–3 h. The solution was then cooled to room temperature, diluted with 100 mL ($5\times$ excess) THF, and passed through an alumina column. The filtrate was concentrated under vacuum to remove THF and the product was precipitated in 200 mL chilled anhydrous diethyl ether. Upon evaporation of ether, a gray-colored PVDF film was obtained. It should be noted that other traditional organic chemistry techniques (e.g. ultracentrifugation, flash chromatography, filtration) can be used to further optimize PVDF separation and purification and reduce these volumes.

Electrochemical Cycling

Galvanostatic cycling experiments were performed to examine the performance of Li half cells containing composite cathode films using recycled PVDF as outlined above and compared to pristine materials. Li half cells were assembled using 2032 coin cells with a Celgard 2325 separator and cycled at C/10 (using the theoretical specific capacity of LCO and NMC, 274 mAh/g and 275 mAh/g, respectively) from 2.7 to 4.2 V vs Li^+/Li to emphasize differences in battery performance. In Figure 4 of the main text both the pristine PVDF and the homemade cells underwent 100 cycles at C/10 between 2.7 and 4.2 V vs Li^+/Li at room temperature. To evaluate the reusability of recovered PVDF, composite cathode films were prepared using commercially available LCO (MTI Corporation, calcined prior to use, carbon black, and PVDF (mass ratio = 80:10:10). Cells containing recycled PVDF were compared with cells containing commercially obtained PVDF (MTI Corporation).

NMR Spectroscopy

^1H NMR spectra were collected on a Bruker DRX 300 spectrometer at room temperature and analyzed in MNOVA. ^1H NMR chemical shift values (δ) were calibrated using the solvent peak (from

residual solvent protons, e.g., 2.51 ppm for DMSO-d_6). For all measurements, a 30° pulse was used for excitation with a recycle delay of 10.5 s (polymer $T_1=300 \text{ ms}$, acetonitrile (ACN) $T_1=7 \text{ s}$). Quantitative analysis was performed to determine unknown PVDF concentrations and ACN was used as an internal standard (100 μL of dilute ACN (2% v/v, 20 μL of ACN in 1 mL DMSO) was added to each sample). Unknown PVDF concentrations were determined by comparison to a four-point standard curve with PVDF concentrations ranging from 1.5–5.5 mg/mL. For each standard, the integral of the PVDF ^1H resonance at 2.91 ppm was divided by the integral of the ACN ^1H resonance at 2.09 ppm and plotted against the known concentrations of PVDF. For all quantitative analyses, a minimum signal-to-noise ratio of 360 was used.

Gel Permeation Chromatography

PVDF samples were analyzed using an EcoSEC RI-UV GPC system equipped with TSKgel SuperH-RC column and a refractive index (RI) detector for determining relative length and dispersity. The measurements were carried out on samples with concentrations of 5 mg/mL that were eluted with DMF containing 0.1 wt% lithium bromide with a flow rate of 0.3 mL/min. Column and RI detector temperature were maintained at $45\text{--}50^\circ\text{C}$ during analysis. GPC samples were prepared by slowly dissolving PVDF in 1 mL mobile phase overnight on a hotplate set at 40°C with gentle stirring. Fully dissolved polymers were slowly filtered through $0.2 \mu\text{m}$ PTFE syringe filters immediately prior to injection. Pristine PVDF binder (MTI Corporation), was run as a reference and is the same material that is used to make our homemade composite films. Thus, direct comparison from these analyses will show whether or not any degradation has occurred during the recovery process. The number-average (M_n) and weight-average (M_w) molecular weights as well as the dispersities (\bar{D}) were estimated using the following series of poly(methyl methacrylate) (PMMA) standards: M_p (peak molecular weight) = 0.55 kg/mol, 0.96 kg/mol, 1.84 kg/mol, 6.10 kg/mol, 13.9 kg/mol, 26.5 kg/mol, 72.0 kg/mol, 146 kg/mol, 265 kg/mol, 504 kg/mol, 964 kg/mol, 1,568 kg/mol. We note that determination of molecular weights from GPC may not be absolutely quantitative because the GPC calibrating agent poly(methyl methacrylate) (PMMA) gives positive RI signal.

Wide-Angle X-Ray Scattering

WAXS for pristine PVDF powder and the recovered, free-standing polymer films was performed on a laboratory-scale system at Columbia University (Ganesha, SAXSLAB) with a Cu $K\alpha$ source ($\lambda=1.54 \text{ \AA}$). A Pilatus 300k detector (Dectris) was used to collect the two-dimensional (2D) scattering pattern with nominal pixel dimensions of $172 \times 172 \mu\text{m}$. Scattering data was obtained upon 30 min exposure at room temperature under vacuum. 2D scattering patterns were integrated using SAXSLAB's saxsui software to obtain $I(q)$ data.

Scanning Electron Microscopy

Samples were mounted on brass shims using carbon adhesive (Electron Microscopy Sciences) and imaged normal to the planar film surface. PVDF polymer powder and films were sputter coated with a gold-palladium alloy using a Cressington 108 Manual Sputter Coater. Top-view images of PVDF microstructure were acquired using a Zeiss Sigma VP Scanning Electron Microscopy (SEM) at an acceleration voltage of 5 keV and an in-lens secondary electron detector, whereas an acceleration voltage of 3 keV was used for imaging active material powders. The working distance for both cases was maintained at $\sim 3\text{--}4 \text{ mm}$. The elemental composition of

the commercial battery cathode materials (recycled) were examined by recording energy dispersive X-ray spectra (EDS).

Powder X-Ray Diffraction

PXRD data of all samples was collected using a PANalytical X'Pert3 Powder diffractometer equipped with a diffracted beam monochromator and a Cu target X-ray source. Samples were evenly dispersed on a zero-background Si plate and sealed within an air-free domed sample holder using Kapton film in the glovebox. Diffraction patterns were collected in the range of scattering angles, 2θ , of 10° – 70° .

Acknowledgements

L.E.M. acknowledges support from startup funds provided by Columbia University and the Columbia University's Provost Grants Program for Junior Faculty who Contribute to the Diversity Goals of the University. R.M. is supported by the U.S. Department of Defense through the National Defense Science & Engineering Graduate (NDSEG) Fellowship Program. We thank Prof. Dan Steingart for helpful discussions and generous donation of Samsung batteries. We thank Columbia University for the support of the Shared Materials Characterization Laboratory and the Soft Matter Characterization Laboratory, which were used extensively in this work.

Conflict of Interest

The authors declare no conflict of interest.

Keywords: direct cathode recycling · HF elimination · lithium-ion batteries · PVDF recycling · PVDF solubility

- [1] Bloomberg, NEF, "Electric Vehicle Outlook", can be found under <https://about.bnef.com/electric-vehicle-outlook/>, 2020 (accessed: 10 March 2020).
- [2] K. Richa, PhD thesis, Rochester Institute of Technology, 2016.
- [3] G. Harper, R. Sommerville, E. Kendrick, L. Driscoll, P. Slater, R. Stolk, A. Walton, P. Christensen, O. Heidrich, S. Lambert, A. Abbott, K. Ryder, L. Gaines, P. Anderson, *Nature* **2019**, 575, 75–86.
- [4] M. Chen, X. Ma, B. Chen, R. Arsenault, P. Karlson, N. Simon, Y. Wang, *Joule* **2019**, 3, 2622–2646.
- [5] L. Chen, X. Tang, Y. Zhang, L. Li, Z. Zeng, Y. Zhang, *Hydrometallurgy* **2011**, 108, 80–86.
- [6] T. Giorgi-Maschler, B. Friedrich, R. Weyhe, H. Heegn, M. Rutz, *J. Power Sources* **2012**, 207, 173–182.
- [7] L.-P. Hi, S.-Y. Sun, Y.-Y. Mu, X.-F. Song, J.-G. Yu, *ACS Sustainable Chem. Eng.* **2017**, 5, 714–721.
- [8] D. A. Ferreira, L. M. Z. Prados, D. Majuste, M. B. Mansur, *J. Power Sources* **2009**, 187, 238–246.
- [9] R.-C. Wang, Y.-C. Lin, S.-H. Wu, *Hydrometallurgy* **2009**, 99, 194–201.
- [10] M. B. J. G. Freitas, V. G. Celante, M. K. Pietre, *J. Power Sources* **2010**, 195, 3309–3315.
- [11] G. Dorella, M. B. Mansur, *J. Power Sources* **2007**, 170, 210–215.
- [12] L. Li, J. B. Dunn, X. X. Zhang, L. Gaines, R. J. Chen, F. Wu, K. Amine, *J. Power Sources* **2013**, 233, 180–189.
- [13] L. Li, J. Ge, F. Wu, R. Chen, S. Chen, B. Wu, *J. Hazard. Mater.* **2010**, 176, 288–293.
- [14] L. Li, J. Lu, Y. Ren, X. X. Zhang, R. J. Chen, F. Wu, K. Amine, *J. Power Sources* **2012**, 218, 21–27.
- [15] L. Sun, K. Qiu, *Waste Manage.* **2012**, 32, 1575–1582.
- [16] G. P. Nayaka, J. Manjanna, K. V. Pai, R. Vadavi, S. J. Keny, V. S. Tripathi, *Hydrometallurgy* **2015**, 151, 73–77.
- [17] G. P. Nayaka, K. V. Pai, J. Manjanna, S. J. Keny, *Waste Manage.* **2016**, 51, 234–238.
- [18] X. Zhang, L. Li, E. Fan, Q. Xue, Y. Bian, F. Wu, R. Chen, *Chem. Soc. Rev.* **2018**, 47, 7239–7302.
- [19] X. Zhang, Q. Xue, L. Li, E. Fan, F. Wu, R. Chen, *ACS Sustainable Chem. Eng.* **2016**, 4, 7041–7049.
- [20] Y. Weng, S. Xu, G. Huang, C. Jiang, *J. Hazard. Mater.* **2013**, 246–247, 163–172.
- [21] B. J. Ross, M. LeResche, D. Liu, J. L. Durham, E. U. Dahl, A. L. Lipson, *ACS Sustainable Chem. Eng.* **2020**, 8, 12511–12515.
- [22] Y. Shi, G. Chen, F. Liu, X. Yue, Z. Chen, *ACS Energy Lett.* **2018**, 3, 1683–1692.
- [23] J. B. Dunn, L. Gaines, J. Sullivan, M. Q. Wang, *Environ. Sci. Technol.* **2012**, 46, 12704–12710.
- [24] F. Arshad, L. Li, K. Amin, E. Fan, N. Manurkar, A. Ahmad, J. Yang, F. Wu, R. Chen, *ACS Sustainable Chem. Eng.* **2020**, 8, 13527–13554.
- [25] E. Fan, L. Li, Z. Wang, J. Lin, Y. Huang, Y. Yao, R. Chen, F. Wu, *Chem. Rev.* **2020**, 120, 7020–7063.
- [26] S. Natarajan, K. Subramanyan, R. B. Dhanalakshmi, A. M. Stephan, V. Aravindan, *Batteries & Supercaps* **2020**, 3, 581–586; *Supercaps* **2020**, 3, 581–586.
- [27] J. E. C. Sabisch, A. Anapolsky, G. Liu, A. M. Minor, *Resour. Conserv. Recycl.* **2018**, 129, 129–134.
- [28] H. Nie, L. Xu, D. Song, J. Song, X. Shi, X. Wang, L. Zhang, Z. Yuan, *Green Chem.* **2015**, 17, 1276–1280.
- [29] L. Li, R. Chen, F. Sun, F. Wu, J. Liu, *Hydrometallurgy* **2011**, 108, 220–225.
- [30] M. Contestabile, S. Panero, B. Scrosati, *J. Power Sources* **2001**, 92, 65–69.
- [31] W. Lv, Z. Wang, H. Cao, Y. Sun, Y. Zhang, Z. Sun, *ACS Sustainable Chem. Eng.* **2018**, 6, 1504–1521.
- [32] B. J. Henry, J. P. Carlin, J. A. Hammerschmidt, R. C. Buck, L. W. Buxton, H. Fiedler, J. Seed, O. Hernandez, *Integr. Environ. Assess. Manage.* **2018**, 14, 316–334.
- [33] X. Zeng, J. Li, L. Liu, *Renewable Sustainable Energy Rev.* **2015**, 52, 1759–1767.
- [34] G. Zhang, Y. He, H. Wang, Y. Feng, W. Xie, X. Zhu, *ACS Sustainable Chem. Eng.* **2020**, 8, 2205–2214.
- [35] Q. Zhang, J. Lu, F. Saito, M. Baron, *J. Appl. Polym. Sci.* **2001**, 81, 2249–2252.
- [36] M. L. O'shea, C. Morterra, M. J. D. Low, *Mater. Chem. Phys.* **1990**, 26, 193–205.
- [37] Y. Chen, N. Liu, Y. Jie, F. Hu, Y. Li, B. P. Wilson, Y. Xi, Y. Lai, S. Yang, *ACS Sustainable Chem. Eng.* **2019**, 7, 18228–18235.
- [38] J. G. Speight, *Chapter Three-Industrial Inorganic Chemistry. Environmental Inorganic Chemistry for Engineers*. Elsevier Inc. **2017**, p. 111.
- [39] M. Ponikvar, Exposure of Humans to Fluorine and Its Assessment, Tressaud, A., Haufe, G. (Eds.), *Fluorine and Health: Molecular Imaging, Biomedical Materials and Pharmaceuticals* (first ed.) Elsevier, Amsterdam **2008**, pp. 488–549.
- [40] J. Diekmann, C. Hanisch, L. Frobose, G. Schalicke, T. Loellhoeffel, A.-S. Folster, A. Kwade, *J. Electrochem. Soc.* **2017**, 164, A6184–A6191.
- [41] D. Song, X. Wang, E. Zhou, P. Hou, F. Guo, L. Zhang, *J. Power Sources* **2013**, 232, 348–352.
- [42] Y. Shi, M. Zhang, Y. S. Meng, Z. Chen, *Adv. Energy Mater.* **2019**, 9, 1900454.
- [43] X. Song, T. Hu, C. Liang, H. L. Long, L. Zhou, W. Song, L. You, Z. S. Wu, J. W. Liu, *RSC Adv.* **2017**, 7, 4783–4790.
- [44] Y. Xu, D. Song, L. Li, C. An, Y. Wang, L. Jiao, H. A. Yuan, *J. Power Sources* **2014**, 252, 286–291.
- [45] D. Song, X. Wang, H. Nie, H. Shi, D. Wang, F. Guo, X. Shi, L. Zhang, *J. Power Sources* **2014**, 249, 137–141.
- [46] "Plastic & Climate: The Hidden Costs of a Plastic Planet", can be found under www.ciel.org/plasticandclimate, **2019** (accessed: 10 March 2020).
- [47] W. W. Y. Lau, Y. Shiran, R. M. Bailey, E. Cook, M. R. Stuchtey, J. Koskella, C. A. Velis, L. Godfrey, J. Boucher, M. B. Murphy, R. C. Thompson, E. Jankowska, A. C. Castillo, T. D. Pilditch, B. Dixon, L. Koerselman, E. Kosior, E. Favoino, J. Gutberlet, S. Baulch, M. E. Atreya, D. Fischer, K. K. He, M. M. Petit, U. R. Sumaila, E. Neil, M. V. Bernhofen, K. Lawrence, J. E. Palardy, *Science* **2020**, 369, 1455–1461.
- [48] D. J. Fortman, J. P. Brutman, G. X. De Hoe, R. L. Snyder, W. R. Dichtel, M. A. Hillmyer, *ACS Sustainable Chem. Eng.* **2018**, 6, 11145–11159.
- [49] A. V. Le, M. Wang, D. J. Noelle, Y. Shi, Y. S. Meng, D. Wu, J. Fan, Y. Qiao, *Int. J. Energy Res.* **2017**, 41, 2430–2438.

- [50] J. C. Barbosa, J. P. Dias, S. Lanceros-Mendez, C. M. Costa, *Membranes* **2018**, *8*, 45.
- [51] A. Lezzi, Polyvinylidene Fluoride Based Coating Technology. ASM Handbook, Volume 5B, Protective Organic Coatings **2015**.
- [52] Method for Purifying Collected NMP Solution and Manufacturing PVDF-NMP Solution Using It. South Korea Patent KR101663481B1, **2016**.
- [53] M. R. M. Abed, PhD thesis, Imperial College of Science, Technology and Medicine, London, **2012**.
- [54] C. Hanisch, W. Haselrieder, A. Kwade, Recovery of Active Materials from Spent Lithium-Ion Electrodes and Electrode Production Rejects. In: Hesselbach, J., Herrmann, C. (Eds.) *Glocalized Solutions for Sustainability in Manufacturing*. Springer, Berlin Heidelberg, pp. 85–89.
- [55] S. Golcuk, A. E. Muftuoglu, S. U. Celik, A. Bozkurt, *J. Polym. Res.* **2013**, *20*, 144.
- [56] I. Terzic, N. L. Meereboer, K. Loos, *Polym. Chem.* **2018**, *9*, 3714–3720.
- [57] Q. Quan, H. Gong, M. Chen, *Polym. Chem.* **2018**, *9*, 4161–4171.
- [58] P. Martins, A. C. Lopes, S. Lanceros-Mendez, *Prog. Polym. Sci.* **2014**, *39*, 683–706.
- [59] R. Gregorio, *J. Appl. Polym. Sci.* **2006**, *100*, 3272–3279.
- [60] D. M. Easterly, B. J. Love, *J. Polym. Sci. Part B* **2004**, *42*, 91–97.
- [61] H. Kim, J. Johnson, L. A. Chavez, C. A. Garcia Rosales, T.-L. Bill Tseng, Y. Lin, *Ceram. Int.* **2018**, *44*, 9037–9044.
- [62] V. F. Cardoso, G. Minas, C. M. Costa, C. J. Tavares, S. Lanceros-Mendez, *Smart Mater. Struct.* **2011**, *20*, 087002.
- [63] R. Magalhaes, N. Duraes, J. Silva, V. Sencadas, G. Botelho, J. L. Gomez Ribelles, S. Lanceros-Mendez, *Soft Mater.* **2011**, *9*, 1–14.
- [64] Y. Jiang, C. Qin, P. Yan, M. Sui, *J. Mater. Chem. A* **2019**, *7*, 20824–20831.
- [65] B. Koo, H. Kim, Y. Cho, K. T. Lee, N. S. Choi, J. Cho, *Angew. Chem. Int. Ed.* **2012**, *51*, 8762–8767; *Angew. Chem.* **2012**, *124*, 8892–8897.
- [66] H. Mendoza, S. A. Roberts, V. E. Brunini, A. M. Grillet, *Electrochim. Acta* **2016**, *190*, 1–15.
- [67] R. E. Ciez, J. F. Whitacre, *Nat. Sustainability* **2019**, *2*, 148–156.
- [68] D. L. Wood, J. D. Quass, J. Li, S. Ahmed, D. Ventola, C. Daniel, *Drying Technol.* **2017**, *0*, 1–11.
- [69] Targray. White Paper: *Hydrophilic Binder Performance in Li-Ion Batteries*, can be found under <https://www.targray.com/articles/hydrophilic-binder>, **2017** (accessed March 10, 2020).
- [70] J. B. Dunn, L. Gaines, M. Barnes, J. Sullivan, M. Wang, United States: N. p., 2012. Web.doi:10.2172/1044525.
- [71] A. Ostermayer, J. Giegrich, *Eco-Profiles of the European Plastic Industry: Polyvinyl Chloride (Emulsion Polymerization)*, The European Council of Vinyl Manufacturers (ECVM) and Plastics Europe. **2006 a**.

Manuscript received: March 9, 2021
Revised manuscript received: March 17, 2021